Spatial distribution and ecological risk assessment of heavy metals in karst soils from the Yinjiang County, Southwest China

Ruiyin Han[1,2] and Zhifang Xu[1,2,3]

[1] Institute of Geology and Geophysics, Chinese Academy of Sciences (CAS), Beijing, China
[2] University of Chinese Academy of Sciences, Beijing, China
[3] Chinese Academy of Sciences, Center for Excellence in Life and Paleoenvironment, Beijing, China

Corresponding author
Zhifang Xu, zfxu@mail.iggcas.ac.cn

ABSTRACT

Background. Soil heavy metals (HMs) under different land-use types have diverse effects, which may trigger the ecological risk. To explore the potential sources of HMs in karst soils, the spatial distribution and geochemical behavior of HMs based on different land-use types are employed in this study.

Methods. Soil samples ($n = 47$) were collected in three suites of karst soil profiles from the secondary forest, abandoned cropland and shrubland in Yinjiang, Southwest China. The concentrations of Ni, Mn, Cr, Pb, Cd and Mo were determined to give a comprehensive understanding of the possible sources of these HMs and evaluate the potential ecological risk in Yinjiang County.

Results. The mean concentrations of HMs in all profiles followed the same order: Mn > Cr > Ni > Pb > Mo > Cd. Meanwhile, the concentrations of most HMs roughly increased with the depth. Additionally, the concentrations of HMs were mostly correlated with soil pH and SOC, rather than with clay and silt proportions. By contrast, with the enrichment factors (EF), geo-accumulation (I_{geo}) and potential ecological risk index (PERI) of HMs in soil under different land-use types, the results indicated that these HMs exhibited non-pollution ($I_{geo} < 0$) and no ecological risk (PERI < 30) to human health in soils of Yinjiang County.

Conclusions. The distribution of HMs is dominated by weathering in the karst area, and the effects of agricultural inputs on the enrichment of soil HMs in Yinjiang County are limited. This further state that the arrangement of the local agricultural structure is reasonable.

INTRODUCTION

Soil acts an important sink of heavy metals (HMs) in the Earth's surface system. There are two ways for soil to accumulate HMs: (i) natural inputs from the weathering of continental rocks, and (ii) anthropogenic sources such as industrial production, atmospheric precipitation and agricultural activities (*Taylor et al., 2010*; *Wei & Yang, 2010*). As a vital

environmental media, soil can be directly affected by human activities, including farming activities, mining development and smelting (*Qiu et al., 2016*; *Skierszkan et al., 2016*; *Wang & Zhang, 2007*). Soil environment, in turn, affects human health in multifarious ways. The poisonous Mo, Cd and Pb metals in soil can be easily absorbed by crops, resulting in a high chronic carcinogenic risk for human beings (*Demir, 2021*; *Xiao et al., 2017*). The intake of proper quantity of HMs is essential for the living organisms growing, whereas the excessive intake of HMs will provoke detrimental effects on vegetation, animals and human bodies (*Sawut et al., 2018*; *Taylor et al., 2010*). The soil adsorption of Cr is limited because Cr is mostly available in water-soluble or exchangeable from in soil (*Liu et al., 1990*). As a migratory pollutant, Cr could very easily affect the resident water environment by polluting groundwater. The compounds of Mn and Ni may also be absorbed by plants and forage crops, ultimately into the body of herbivores and humans (*Bashir, Ahmad & Khan, 2020*; *Fardous et al., 2011*). Excessive HMs and their interaction can also aggravate bioavailability and ecological risk (*Lago-Vila et al., 2017*). Accordingly, the accumulation degree of HMs (*e.g.*, Mn, Ni, Cr, Pb, Cd and Mo) in soils can indicate soil environment pollution level and ecological risk.

The information containing in a suit of soil profile can reflect the soil physical and chemical processes at a specific site (*Liu et al., 2016b*; *Vodyanitskii & Yakovlev, 2011*). Previous researches have mainly focused on the spatiotemporal variations and the contamination of HMs in human-affected regions, for examples, sewage irrigation area, polluted farmland and mining area (*Khanal et al., 2014*; *Kong et al., 2018*; *Liu et al., 2016a*; *You et al., 2015*). However, the studies of HMs characteristics in soil profile were mostly aimed at a single land-use type (*Balabane et al., 1999*; *Vodyanitskii & Yakovlev, 2011*). Little is known about the vertical distribution of HMs based on different land-use types under the same geological background, especially for the soils in the karst area. The manner and degree of human disturbance are closely associated with land-use types, which can affect the spatial distribution of HMs in soil profiles. The research on HMs characteristics in soil profiles under different land-use types is almost negligible and thus poorly documented. Accordingly, it is of vital importance to investigate the vertical characteristics of HMs under different land-use patterns and human interferential degrees in the karst regions.

The karst ecosystem belongs to a highly fragile ecosystem that can be easily affected by anthropogenic activities (*Han et al., 2020*). The slight discrepancy in different soil types may be more prominent in the karst region (*Liu et al., 2013*; *Parise, De Waele & Gutierrez, 2009*). In the karst region, the high-rate of rock weathering and low-rate of soil formation can result in a strong spatial of soil distribution and chemical composition in soils (*Gao et al., 2013*). Even though at the similar depth, the physicochemical properties and HMs concentrations in the soils derived from different locations likely show substantial discrepancies (*Gregorauskiene & Kadunas, 2006*). Moreover, the soil was mainly developed from limestone in the karst area of southwest China, and sizable amounts of HMs were released due to its unique geochemical process (*Wen et al., 2020*; *Zhao et al., 2015*). Naturally, the concentrations of Mn, Ni, Cr, Pb, Cd and Mo in karst soils are higher than other area which are not developed from limestone (*Wen et al., 2020*). The migration ability of HMs is stronger with high porosity and heterogeneous distribution in karst
soil (*Tao et al., 2020*). The high concentrations of HMs are harmful to the large soil environment area through surface water and groundwater flow due to the unique hydraulic and hydrogeological characteristics of karst area (*Huang et al., 2020*; *Reimann & Caritat, 2000*). Therefore, it is necessary to analyze the behavior of HMs in the karst area showing potentially higher background concentration.

In Yinjiang County, in addition to weathering and pedogenic processes, agricultural activities play a significant role in regulating the geochemical behaviors of HMs in soils (*Huang et al., 2017*; *Xu et al., 2017b*). Therefore, the purposes of this study were to: (1) explore the vertical distribution of HMs in the profiles under different land-use types; (2) determine the influence of rock weathering processes and anthropogenic inputs on the distribution of HMs in the soils under different land-use types; and (3) evaluate the ecological risks of HMs in karst areas by the enrichment factor (EF), geo-accumulation index (I_{geo}) and potential ecological risk index (PERI). This study is desirable to extend the knowledge of the migration process of HMs in soil under different land-use types soils in karst area and evaluate the possible influence of interferential degrees from human. The HMs results in this study can supply the data supporting soil management for soil quality and sustainability.

MATERIALS & METHODS

Study area

The study area is located in the Yinjiang County (Fig. 1), a karst region in Guizhou Province, of Southwest China. The study area lies between 27°35′–28°21′N and 108°18′–108°48′E, with above 454,000 permanent resident population. The Yinjiang County is dominated by the subtropical monsoon climate, with the variation in temperature from −9 °C to 39.9 °C (*Xu et al., 2017b*). Rainfalls are mainly concentrated from April to September, with the annual precipitation of 1,057–1,268 mm (*Xu et al., 2017a*). The rock exposed in the Yinjiang County is dominated by the Permian and Triassic carbonates, with a rocky desertification area of 11783.06 hm^2 (*Huang et al., 2017*; *Li, 2018*). The elevation decreases from southeast to northwest, a typical karst trough valley with a relative elevation exceeding 2,000 m (*Li, 2018*). The study area is far away from urban cities and diggings and mostly covered by cropland (*Huang et al., 2017*). The agricultural areas in Yinjiang County accounted for nearly 30% of the total area with the main crops being corn and sweet potatoes (*TBS, 2017*), and the forest area accounted above 60% of the total area with the dominant vegetation of *Platycarya strobilacea Sieb.et Zucc., Melia azedarach L.* and *Quercus fabri Hance*. The vegetation of shrubland is mainly cultivated with *Pyracantha fortuneana, Castanea mollissima, Lindera communis*. The main soil types of Yinjiang county are Mollic Inceptisols *Soil Survey Staff, 2010*, which are calcareous soils derived from limestone rocks.

Sample collection

A total of 47 soil samples were collected during September 2016 in the Yinjiang County, from the three soil profiles in secondary forest land (T1, $n = 20$), abandoned cropland (T2, $n = 16$) and shrubland (T3, $n = 11$), respectively. Due to the strong spatial heterogeneity
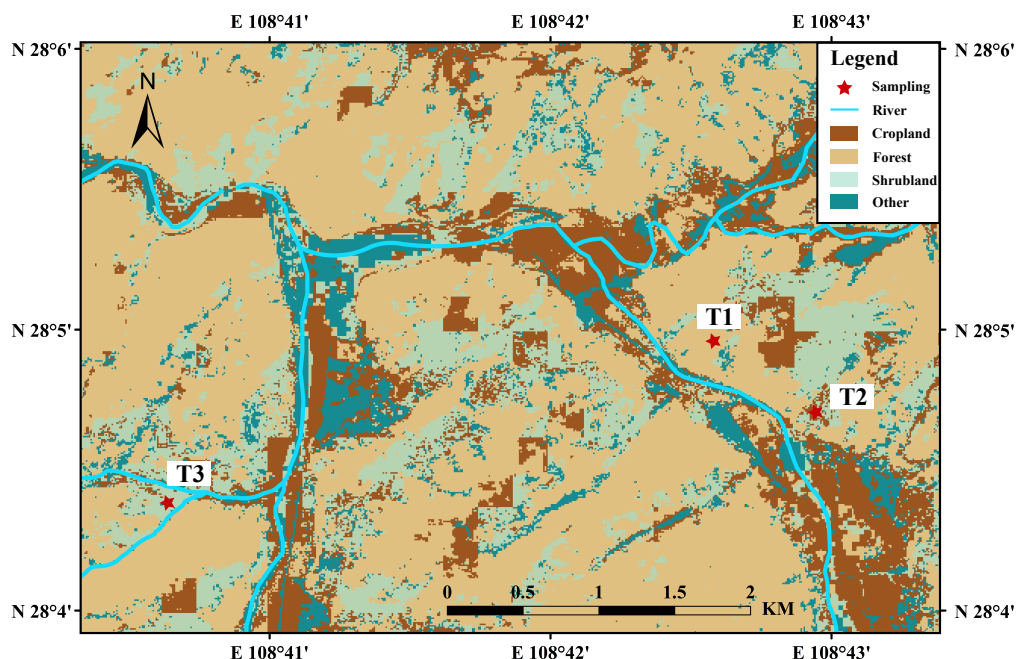
Figure 1 Land-use types profiles sites and in the study area.

in soil properties, particularly at the vertical direction, three duplicate soil profiles of less than 1 meter were selected at each sampling sites. Moreover, the results were presented as an average of three samples derived from the three duplicate profiles at the same depth in the present study. The detailed descriptions of soil profiles are shown in Table 1.

Soil analyses

Soil samples were air-dried and sieved through a two mm sieve after removing big litters and stones. For subsequent analysis, soils were entirely grounded to around 200 mesh. Soil particles were categorized into three groups including clay (<2 μm), silt (2 μm to 50 μm) and sand (50 μm to 2,000 μm) according to USDA Soil Taxonomy (Soil Survey Staff, 2010). Soil pH was measured using glass electrode in the 1:2.5 soil–water suspension with a precision of ±0.05. Soil powders were digested with HNO_3–HF–$HClO_4$ (*Li et al., 2022*; *Li et al., 2020*; *Liu, Han & Li, 2021*). The concentrations of Al, Cr, Mn were determined by ICP–OES (Optima 5300DV; Perkin Elmer, Waltham, MA, US) and the concentrations of Ni, Mo, Cd, Pb were analyzed by ICP–MS (Elan DRC–e; Perkin Elmer, Waltham, MA, US) in the Institute of Geographic Sciences and Natural Resources Research, CAS at precision ±5%. Quality control and quality assurance were performed by the procedural blank and standard reference material (GBW07447 and GBW07449).

Data calculation
Index of enrichment factor

As the indicator in various environmental media, the enrichment factor (EF) and the Geo–accumulation Index (I_{geo}) widely employs to quantify the accumulation and contamination

Table 1 Geographic information, dominant vegetation and profile characteristic at the soil sites.

Profile	Location	Altitude (m)	Thickness (cm)	Land-use types and primary vegetation	Profile descriptions
Secondary forest (T1)	28°04′57.64″N 108°42′31.01″E	838	160	Subtropical evergreen broad–leaved secondary forest, interspersed with *Platycarya strobilacea Sieb.et Zucc., Melia azedarach L., Quercus fabri Hance. etc.*	0–5 cm: Gray soil, abundant plant roots, and debris. 5–85 cm: Yellow clay and silt, few small stone particles. 85–160 cm: Relatively uniform brawn to red soil, connect to bedrock.
Abandoned cropland (T2)	28°04′48.35″N 108°42′58.22″E	892	130	Sloping farmland, cultivation history is about 50 years, the main crops are corn and potatoes, which have been abandoned 3 years before sampling	0–25 cm: Yellow soil, few plant residues, and small stone particles. 25–110 cm: Relatively uniform yellow fine silt. 110–130 cm: Yellow brawn to red brawn soil, more stones.
Shrubland (T3)	28°04′22.68″N 108°40′37.62″E	776	70	Native shrub grass slope, the main plants are *Pyracantha fortuneana, Castanea mollissima, Lindera communis,* and interspersed with less *Cunninghamia lanceolata, Pinus massoniana Lamb, etc.*	0–10 cm: Black soil, abundant humus, few stones. 10–25 cm: Gray soil, abundant stones. 25–70 cm: Yellow soil, few stones, connect to bedrock.

Table 2 The classification of EF values and I_{geo} values.

EF	Soil quality	I_{geo}	Soil quality
EF < 2	Negligible enrichment	$I_{geo} < 0$	Non-pollution
$2 \leq$ EF < 5	Moderate enrichment	$0 \leq I_{geo} < 1$	Minor pollution
$5 \leq$ EF < 20	Significant enrichment	$1 \leq I_{geo} < 2$	Moderate pollution
$20 \leq$ EF < 40	Severe enrichment	$2 \leq I_{geo} < 3$	Moderate to severe pollution
EF $\geq$ 40	Extremely severe enrichment	$3 \leq I_{geo} < 4$	Severe pollution
		$4 \leq I_{geo} < 5$	Severe to extreme pollution
		$I_{geo} \geq 5$	Extreme pollution

of metallic elements through calculating the soil exchangeable fractions (*Barbieri, 2016*; *Zeng, Han & Yang, 2020*).

The indexes of EF are usually calculated by the normalized concentration of a metal relative to its reference concentration (*Barbieri, 2016*; *Mazurek et al., 2017*). The representative element used in several studies is Al due to its insusceptible property (*Ackermann, 1980*; *Blaser et al., 2000*). The formula of EF is shown as:

$$EF = \frac{(M/Al)_S}{(M/Al)_B} \tag{1}$$

where M means the concentrations of metal (mg kg^{-1}), and S means soil samples. And calculated the $(M/Al)_B$ ratio based on the HMs and Al values in the average soils of Guizhou Province (*China Environmental Monitoring Station, CEMS)(1990*). *Barbieri (2016)* categorized the EF values into five grades (Table 2).

Index of Geo–accumulation

The Geo–accumulation Index (I_{geo}) is extensively employed to evaluate anthropogenic contamination levels (*Nazeer, Hashmi & Malik, 2014*; *Zoller, Gladney & Duce, 1974*). *Müller (1971)* defined the formula of I_{geo} as:

$$I_{geo} = \log2(S_M/1.5R_M) \tag{2}$$

where S_M represents the concentrations of HMs in samples; R_M represents the reference value for HMs in Guizhou Province (*China Environmental Monitoring Station, CEMS)(1990)*, and the constant 1.5 is applied to eliminate the lithological fluctuations (*Barbieri, 2016*). Accordingly, the values of I_{geo} are separated into seven classes (Table 2) from non-pollution to extreme pollution (*Müller, 1971*).

Index of potential ecological risk

Hakanson (1980) originally proposed the potential ecological risk index (PERI) to effectively appraise the ecological risk of HMs in sediment or soil. Extensive studies have applied PERI to estimate the potential ecological risk and pollution level triggered by single or multiple HMs (*Aboubakar et al., 2021*; *Gujre, Rangan & Mitra, 2021*; *Sun et al., 2010*). The (3)–(5) to calculate PERI are as:

$$C_c^i = C_s^i/C_r^i \tag{3}$$

$$E_f^i = T_f^i \times C_c^i \tag{4}$$

$$RI = \sum_{i=1}^{n} E_f^i \tag{5}$$

where C_c^i indicates the contaminated factor of each heavy metal, C_s^i represents the measured concentration of HMs in soils, C_r^i represents the reference value for HMs in the average soils of Guizhou Province (*China Environmental Monitoring Station, CEMS)(1990)*. E_f^i indicates the potential ecological risk of each heavy metal, T_f^i represents the toxic response factor of respective HMs, and RI indicates the comprehensive potential ecological risk of soil HMs (*Hakanson, 1980*). T_f^i values of Mn, Cr, Pb, Ni and Cd were obtained from *Xu et al. (2008)* and were 1, 2, 5, 5, 30, respectively. Unfortunately, the toxicity response factor of Mo is indefinite.

Based on the contaminated degree of single heavy metal, the values of C_c^i and E_f^i are classified into five classes and the values of RI are divided into 4 classes by the comprehensive value of the PERI of multiple HMs (*Gujre, Rangan & Mitra, 2021*; *Qiu et al., 2016*). The specific evaluation indicators and classes are shown in Table 3.

The relationship between different HMs and soil properties was identified by linear-regression analysis, with the determination of the coefficient R and *p*-values by SPSS 25.0 (IBM SPSS Statistics, Chicago, IL, US). The graphics were completed by Origin 2017 (OriginLab, Northampton, MA, USA).
Table 3 The corresponding relationships of C_c^i, E_f^i, RI, and contaminated degree.

C_c^i	Contaminated degree	E_f^i	Contaminated degree	RI	Contaminated degree
$C_c^i \leq 0.7$	Great	$E_f^i < 40$	Slight ecological risk	RI < 150	Slight ecological risk
$0.7 < C_c^i \leq 1.0$	Safety	$40 \leq E_f^i < 80$	Moderate ecological risk	$150 \leq RI < 300$	Moderate ecological risk
$1.0 < C_c^i \leq 2.0$	Slight contamination	$80 \leq E_f^i < 160$	High ecological risk	$300 \leq RI < 600$	High ecological risk
$2.0 < C_c^i \leq 3.0$	Moderated contamination	$160 \leq E_f^i < 320$	Heavy ecological risk	$RI \geq 600$	Heavy ecological risk
$C_c^i > 3.0$	Heavy contamination	$E_f^i \geq 320$	Extremely ecological risk		

RESULTS

Soil properties

Soil properties (*e.g.*, soil pH and soil particle distribution) are the influencing factors that regulate the concentrations of HMs in natural soils (*Wang & Zhang, 2007*; *Zhang et al., 2018*). The variations of soil properties in all profiles are summarized in Table 4. The values of soil pH T1 profile: 7.1–7.9, T2 profile: 4.8–5.2 and T3 profile: 6.3–7.0) in the three profiles have been reported by *Han & Xu (2021)*. Soil silt particle accounted for the largest portion (mean: 85.87% in T1profile; 75.12% in T2 profile; 85.25% in T3 profile), and the second largest was clay (mean: 12.96% in T1profile; 15.50% in T2 profile; 12.09% in T3 profile) in all profiles (*Han & Xu, 2021*). The contents of soil SOC in three profiles ranged from 0.38% to 4.2% in T1 profile, 0.51% to 1.7% in T2 profile and 0.76% to 10.8% in T3 profile.

HMs in the soil profiles

The vertical distributions of the six HMs (Mn, Ni, Cr, Pb, Cd and Mo) in the three soil profiles under different land-use types are presented in Fig. 2, and the concentration data are shown in Table 4. The concentrations of all HMs in Yinjiang County were higher than those in the upper continental crust but lower than the values from the Draft soil screening guidance reported by the EPA (*OSWER 1993*; *Rudnick & Gao, 2003*). Most of the concentrations of HMs are lower than the average soils of Guizhou Province (*China Environmental Monitoring Station, CEMS)(1990)*. The high geological background values of HMs may be related to the regional geochemistry and the endogenous influence of the pedogenesis process in the Guizhou Karst area (*Chen et al., 2019*). A large amount of HMs is released into soils during the weathering of carbonate rocks, causing HMs "concentrated" in soil (*Wu et al., 2020*). The concentrations of metals in all profiles decreased in the following order: Mn (400.43 mg/kg) > Cr (57.28 mg/kg) > Ni (35.85 mg/kg) > Pb (25.34 mg/kg) > Mo (1.87 mg/kg) > Cd (0.33 mg/kg). The concentrations of most HMs in the T1 profile under secondary forest were the highest in the three profiles. The concentrations of most HMs tended to be similar in the bottommost soil

Indexes of ecological risks assessment

Based on the calculation, the EF values of most HMs in soils from three profiles were less than 2. However, the EF values of Ni ranged from 2.16 to 3.90 in the T1 profile and from 1.89 to 2.86 in the T3 profile. The EF values of Pb were greater than 2 in more than one third of the T1 profile, while the EF > 2 was found in the bedrock. Except the sample at

Table 4 **Soil properties and HMs concentrations (mg/kg) in soil samples of the three profiles.** The data of soil pH and soil particle proportion were reported by *Han & Xu, (2021)*.

Profiles	Depth (cm)	pH	SOC (%)	Clay (%)	Silt (%)	Sand (%)	Cr	Mn	Mo	Ni	Pb	Cd
	0	7.2	4.22	13.58	83.97	2.45	79.75	683.8	2.92	41.47	31.73	0.83
	5	7.7	1.73	14.34	84.31	1.35	81.66	642.6	3.12	40.38	28.81	0.70
	10	7.7	1.63	13.38	84.74	1.88	84.42	694.6	3.52	40.47	30.24	0.69
	15	7.7	1.27	14.68	84.34	0.98	76.58	668.9	2.78	37.73	27.59	0.46
	20	7.7	0.85	12.92	85.79	1.29	80.77	626.0	2.17	39.51	28.64	0.35
	30	7.7	0.75	14.41	84.46	1.13	74.99	606.8	2.17	38.23	28.16	0.34
	40	7.9	0.76	15.41	83.92	0.67	73.59	583.5	1.97	40.42	28.69	0.33
	50	7.9	0.94	13.99	85.07	0.94	61.94	557.6	1.67	34.36	24.19	0.32
Secondary forest (T1)	60	7.8	0.71	14.09	84.93	0.99	62.86	647.6	1.86	41.48	29.06	0.33
	70	7.5	0.71	15.99	83.30	0.72	50.45	447.6	1.95	41.57	29.70	0.34
	80	7.7	0.48	14.55	84.82	0.63	55.69	397.5	1.77	40.63	28.23	0.28
	90	7.5	0.41	12.38	86.70	0.92	54.19	342.9	2.24	47.32	28.43	0.24
	100	7.3	0.46	12.60	86.54	0.86	59.71	395.2	2.02	46.24	28.56	0.27
	110	7.3	0.39	12.66	85.79	1.55	56.82	417.2	1.60	41.61	27.37	0.29
	120	7.2	0.38	11.83	87.65	0.52	58.06	454.1	1.67	44.05	29.20	0.31
	130	7.1	0.40	11.00	87.90	1.09	57.14	433.5	1.71	48.48	29.44	0.31
	140	7.1	0.60	10.56	88.42	1.02	67.33	475.9	2.23	55.50	33.62	0.37
	150	7.2	0.47	9.07	88.96	1.97	63.65	507.8	2.28	54.06	34.85	0.34
	160	7.3	0.52	8.71	89.88	1.41	59.29	368.9	2.04	49.50	32.28	0.32
Bedrock							26.57	26.57	85.20	1.14	12.16	8.10
	0	4.8	1.77	10.12	75.46	14.43	59.05	298.8	1.37	31.21	29.60	0.45
	5	4.8	0.70	15.16	72.77	12.08	54.28	258.2	1.05	30.93	25.53	0.31
	10	4.9	0.70	14.05	75.12	10.83	53.73	283.9	1.04	28.91	25.51	0.30
	15	4.8	0.59	12.94	68.65	18.42	46.58	360.5	0.93	29.21	25.79	0.29
	20	5.0	0.58	14.10	75.28	10.63	51.29	331.9	0.91	28.39	25.05	0.26
	30	5.0	0.57	14.30	75.84	9.87	50.18	320.1	0.83	26.98	24.06	0.22
Abandoned cropland (T2)	40	5.1	0.57	16.12	75.86	8.02	49.89	328.3	0.83	27.69	24.00	0.23
	50	5.0	0.55	16.26	75.49	8.25	49.81	323.5	0.73	27.59	22.32	0.21
	60	5.1	0.57	17.90	74.49	7.61	44.70	311.7	0.74	26.07	22.76	0.22
	70	4.8	0.68	16.23	78.19	5.58	49.36	343.0	0.82	27.43	23.08	0.21
	80	4.8	0.73	17.04	77.30	5.66	53.41	314.4	0.81	26.88	23.59	0.19
	90	4.9	0.66	17.40	78.42	4.18	57.03	331.8	0.82	29.54	23.79	0.18
	100	4.9	0.83	16.37	79.63	4.00	49.92	315.8	0.84	26.71	22.94	0.21
	110	5.2	0.51	14.74	73.31	11.95	56.80	370.9	0.79	39.10	34.42	0.23
	120	5.1	0.53	17.82	73.61	8.57	61.58	778.4	0.79	42.00	31.85	0.19
	130	5.1	0.53	17.47	72.50	10.03	54.55	527.2	0.77	42.67	30.06	0.19
	0		10.82				44.23	224.2	2.44	22.86	22.68	0.54
	5	6.3	7.07	10.45	85.99	3.56	41.27	208.6	2.48	24.51	20.71	0.44
	10	6.3	4.82	10.79	85.93	3.28	42.59	234.3	2.65	26.01	21.34	0.43
	15	6.4	3.91	12.16	85.10	2.75	39.97	164.6	2.05	20.63	14.80	0.25

Table 4 (*continued*)

Profiles	Depth (cm)	pH	SOC (%)	Clay (%)	Silt (%)	Sand (%)	Cr	Mn	Mo	Ni	Pb	Cd
Shrubland (T3)	20	6.5	2.72	12.13	85.56	2.31	45.64	194.7	2.43	24.39	3.92	0.33
	30	6.6	1.90	13.33	84.35	2.32	47.41	215.7	3.02	29.76	17.58	0.34
	40	6.8	1.06	13.30	84.24	2.46	53.08	247.5	3.49	35.38	12.55	0.28
	50	7.0	0.84	12.87	85.26	1.87	52.80	236.7	3.84	37.69	19.47	0.26
	60	7.0	0.76	11.36	86.96	1.68	51.78	258.8	3.24	40.40	20.11	0.24
	70	7.0	0.90	12.39	83.90	3.71	57.70	283.8	2.55	37.07	14.14	0.25
Bedrock							26.49	62.69	0.60	9.20	4.17	0.06

the 40 cm depth in the T3 profile, the I_{geo} values of all HMs in soils were lower than 0. Excluding for the C_c^i values of Mo, Ni and Cd in the T1 profile and Mo in the T3 profile were greater than 1, the C_c^i values of other HMs in soils were less than 1. Moreover, most soils showed that values of C_c^i were less than 0.7, especially in the T2 profile. The RI values reveal that Cr, Mn, Ni, Pb and Cd were of slight ecological risk (RI < 60) in the three profiles.

DISCUSSION

Effects of soil particles on HMs

Generally, HMs concentrations are significantly correlated with soil particle distribution (*Probst et al., 2003*). The higher concentrations of HMs in soil are always related to a larger proportion of clay because of the larger specific surface, which tend to increase the absorption capacity of HMs (*Jaradat et al., 2009*). Although the clay contents in the T2 profile was relatively high, the study area soils were silt loamy texture and the clay contents were lower than 20% in three profiles. The adsorption capacity for the HMs is relatively weak.

The phenomenon of the rapid vertical migration of water during irrigation and rainfall was always found in cropland due to higher heterogeneity in cropland soil properties such as preferential flows (*Brusseau & Rao, 1990*). Clay is an important carrier of HMs. Thus, the preferential flow also promotes the translocation of adsorbed HMs by affecting the migration of fine particles (*Zhang, 2005*). In the process of transporting the solution by the preferential flow in soil profile, the chemical composition is stable (*Zhang et al., 2016a; Zhang et al., 2016b*). In recent years, several studies have found that heavy metals migrate rapidly from the soil surface to the deep soils through the soil preferential flow (*Knechtenhofer et al., 2003; Zhang et al., 2016a; Zhang et al., 2016b*). The preferential flow might affect the vertical migration of HMs in the T2 profile. In contrast, some studies suggest that the contribution of preferential flow in HMs migration is limited (*Allaire et al., 2002; Zhang et al., 2016b*). We also observed weak correlation between the size distributions of soil particles and HMs concentrations in this study. It can be inferred that the effect of soil particles is limited on the distribution of HMs in the study soils.
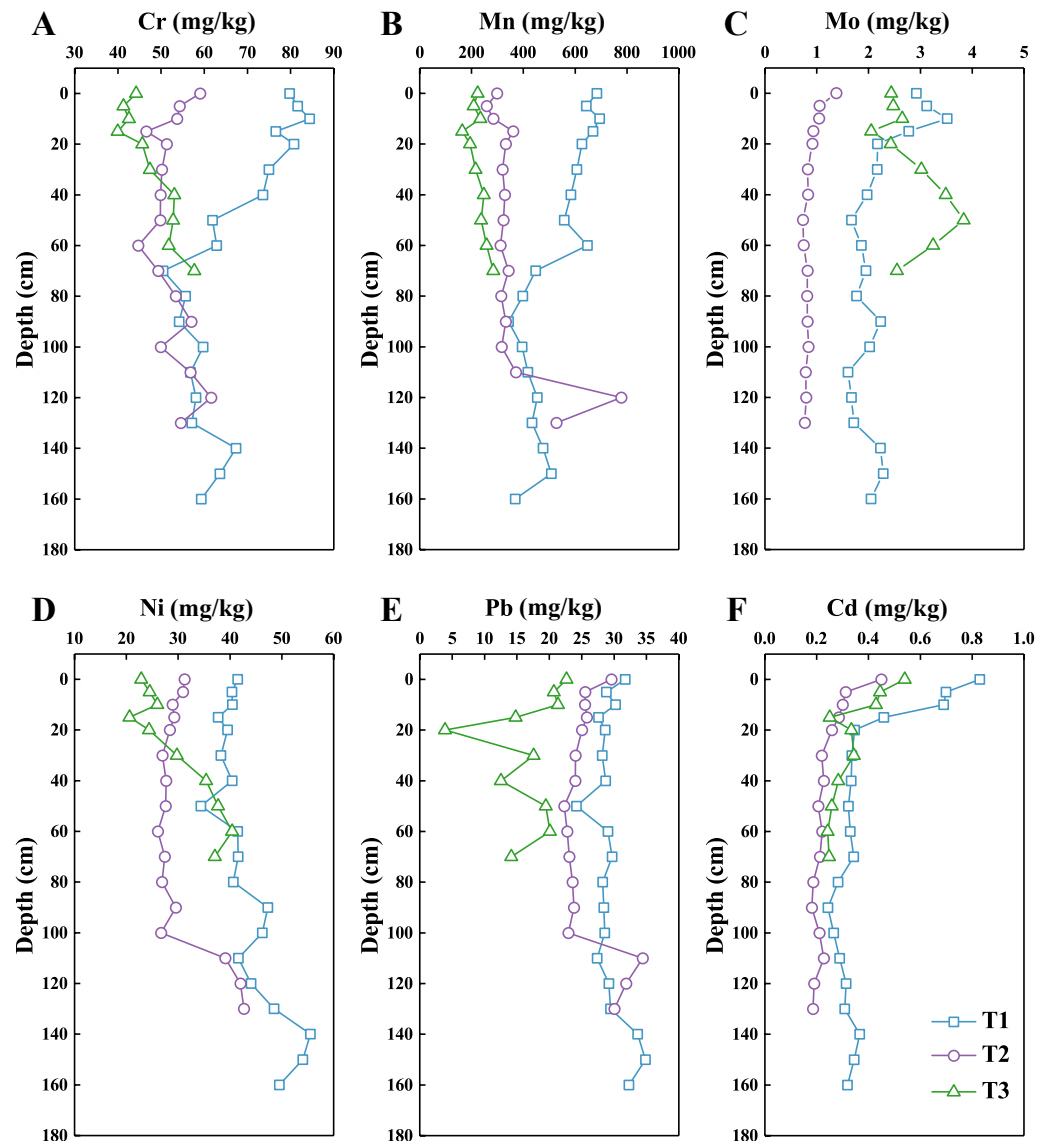
Figure 2 Vertical variation of HMs in the three soil profiles, including Cr (A), Mn (B), Mo (C), Ni (D), Pb (E), and Cd (F).

Effects of soil organic carbon on HMs

SOC is one of the most important properties affecting HMs as the humus could easily coordinate or chelate with HMs by some functional groups (*Dijkstra, 1998*). The correlation analysis between SOC and HMs in 0–30 cm soil layers are presented in Fig. 3. Many studies indicated that the concentrations of HMs show a positive correlation with SOC in the various types of soils including in karst area (*Balabane et al., 1999*; *Mazurek et al., 2017*; *Zhang et al., 2019*). HMs can easily form stable compounds with the soil organic matter (SOM) (*Mazurek et al., 2017*). For example, there was strong correlations between SOC and Pb, Cd in the T1 profile (Figs. 3E, 3F), Cr, Mo, Pb, Cd in the T2 profile (Figs. 3A, 3C,
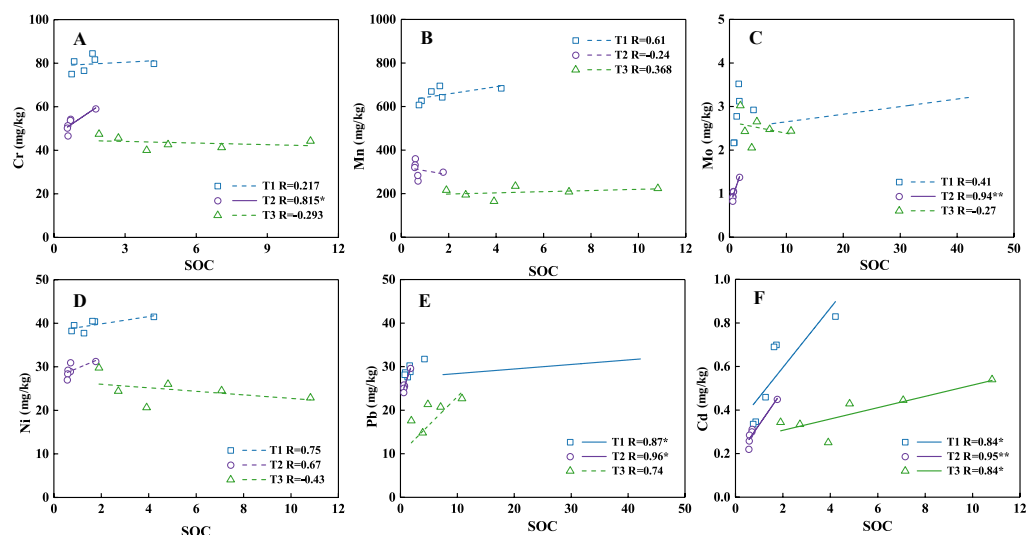
Figure 3 **Correlation analysis of Cr (A), Mn (B), Mo (C), Ni (D), Pb (E), and Cd (F) with soil SOC in 0–30 cm of the three profiles.** Asterisks: ** represents $p < 0.01$; * represents $p < 0.05$.

3E, 3F), and Cd in T3 profile (Fig. 3F). The contents of SOC in shrubland are possibly enriched in the surface soil, and decrease obviously with the depth in the surface soil due to grazing (*Hiernaux et al., 1999*). This phenomenon was also found in T3 profile, and the highest content of SOC was found in T3 profile. However, the distribution of SOC contents in the T2 profile is almost constant. And the contents of HMs almost have no fluctuations which are similar with the distribution of SOC in T2 profile, and present the great correlation between the contents of HMs and SOC. Generally, the content of SOC recovering difficultly in the abandoned cropland for the short term (*Liu, Han & Li, 2021*). The concentrations of HMs almost fluctuated moderately in the T2 profile (abandoned cropland), which may have resulted from the distribution of SOC.

The HMs can be strongly complexed with the organic matter because of the negative charges on its surface (*Marks et al., 2015*). The chelates formed by HMs and organic compounds may increase the availability of metals to plants or reduce their bioavailability to regulate the activities of HMs in soil (*Dijkstra, 1998*; *Zhang et al., 2018*). The absorption capacity of SOC to Cd, Mo and Pb is relatively large, thus may reduce the migration and increase the accumulation in soil (*Dumat et al., 2006*). However, most of the complexes formed by organic matter and Ni are humic acid, which will reduce the content of Ni in soil (*Chimitdorzhieva, Nimbueva & Bodeeva, 2012*). Therefore, the effects of SOC on HMs distribution in soils under different land-use types are mixed. There are multiple factors acting on the distribution of HMs. While the SOC has an important effect, it may not be the dominant factor.

Effects of soil pH on HMs

The concentrations of the six HMs were positively correlated with soil pH, and their correlation analysis is presented in Fig. 4. In the natural environment, the geochemical
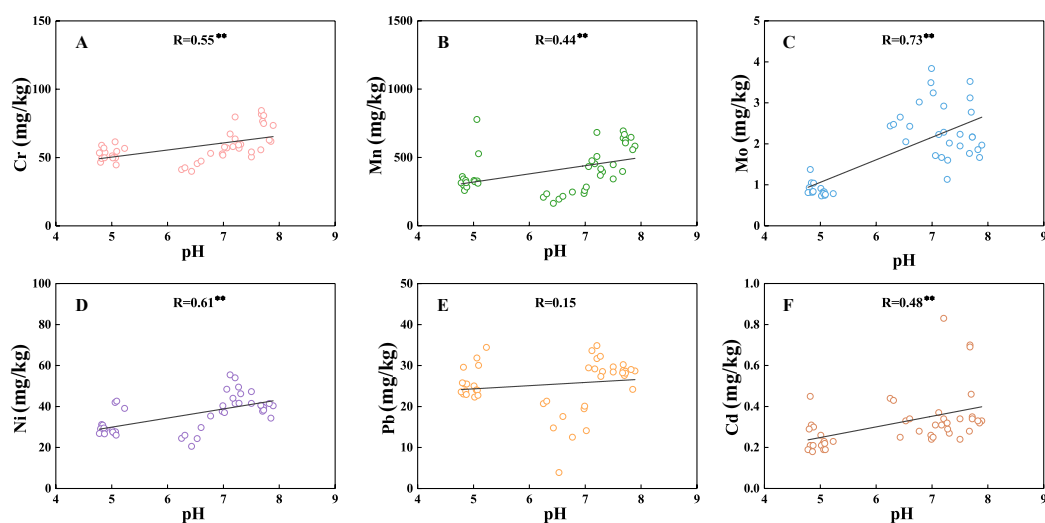
Figure 4 **Correlation of soil pH with Cr (A); (B) Mn; (C) Mo; (D) Ni; (E) Pb; (F) Cd in all soils.** Asterisks: ** represents $p < 0.01$; * represents $p < 0.05$.

behaviors of trace elements are dominantly affected by pH (*Yang et al., 2018*). The changes of soil pH will directly or indirectly affect the soil adsorption of HMs by affecting the stability of complexes, oxide and organic material surface negative charge, hydrolysis of HM ions, the formation of ion pairs, *etc.* (*Rieuwerts et al., 1998*; *Sauvé, McBride & Hendershot, 1997*). The negative charge on the organic matter and clay minerals surface is likely to increase with a high pH, which further enhances the adsorption capacity and the complexes stability of HMs (*Markiewicz-Patkowska, Hursthouse & Przybyla-Kij, 2005*; *Semerjian & Ayoub, 2003*). In addition, HMs will enrich in soil under high pH environment because of decreasing metal availability (*Sparks, 2003*). Generally, the distribution of HMs is mainly controlled by adsorption reaction under acidic conditions, while the precipitation reaction of HMs and hydroxides or carbonate account for a dominant proportion in medium-alkaline conditions (*Ottosen, Hansen & Jensen, 2009*). The relationship between Cr, Mo, Mn, Ni and Cd and soil pH presented similar relation under three soil profiles. With the lower pH and SOC content, the adsorption capacity of soil to HMs is lower in the T2 profile. The soil pH values and concentrations of HMs in the T1 profile are the highest. The soil pH possibly plays an important role in regulating the concentrations of HMs in the T1 profile. It should be considered that the relationship of Pb and soil particle distribution, SOC, soil pH is weak. Result showed that the Pb were slightly enriched in the topsoil (0–5 cm) of three profiles, which may be related to the atmospheric deposition or fertilizer usage (*Kong et al., 2018*).

Soil contamination assessment

The enrichment factors (EF) of HMs in the soils are quantified and displayed in Fig. 5. The mean EF values of most HMs in soils were less than 2, indicating that the enrichment of HMs in most soils was negligible. It is estimated that the characteristic of the geological material may regulate the HMs concentrations, and non-natural sources may contribute
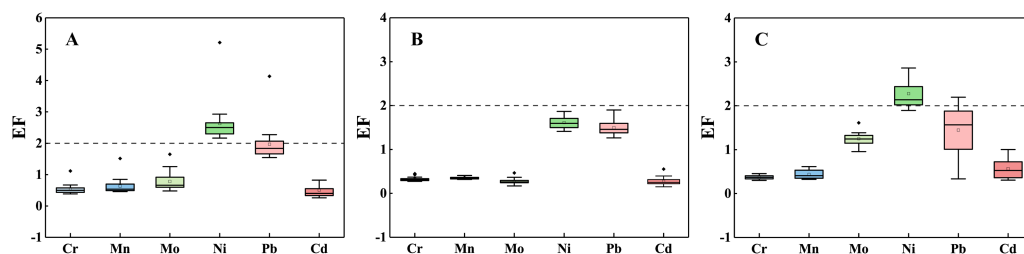
Figure 5 Variation of each EF$_{HMs}$ value in the soils, including T1 profile (A), T2 profile (B), T3 profile (C).

less. Only the EF values of all HMs in the soils of the T2 profile were less than 2. The agricultural activities may be limited to the accumulation of HMs in the T2 profile soil. The higher EF values of Ni in the T1 and T3 profiles indicate that the element Ni was moderately enriched in the T1 and T3 profiles. The Ni concentrations in most soils are close to the background value of Guizhou Province. The difference among the three profiles may be related to the SOC. The study shows that the content of organic matter in abandoned farmland is significantly lower than that in normal vegetation-covered soil, furthermore, the content of SOC in soils will not return to the normal level in a short time after land abandoned (*Liu, Han & Li, 2021*). The EF higher values of Pb in the T1 profile suggest that the Pb of T1 profile are derived from weathering. The EF values of Pb greater than 2 was found in the shallow soil (0–5 cm) of the T3 profile, which may be caused by atmospheric deposition (*Zhang et al., 2016a*). Furthermore, the shallow soil is rich in organic matter which has better adsorption of Pb (*Harter & Naidu, 1995*).

The mean values of the geo-accumulation Index (I_{geo}) of the six HMs at 0–10 cm, 10–20 cm, 20–30 cm, 30–50 cm depths under diverse land-uses are presented in Fig. 6. The I_{geo} values of HMs in soils were lower than 0 in most layers, indicating that the three soil profiles were possibly not polluted by anthropogenic source (*Muller, 1969*). However, comparing the distributions of HMs concentrations in the three profiles, the agricultural activities at the T2 profile and the goats' grazing activities near the T3 profile show limited impact on the HMs in soil.

Ecological risk assessment

The calculated contaminated factor (C_c^i) values of six HMs in the Yinjiang County are presented in Fig. 7. According to the classification of C_c^i values by *Qiu et al. (2016)*, the pollution degree of HMs in the research profile is only slight pollution at most, such as Ni in the T1 profile (the highest value: 1.42) and Mo in the T3 profile (the highest value: 1.60). Since the secondary forest has no disturbance from human activities, it can be speculated that the higher Ni concentrations in the T1 profile may correspond to natural factors such as the weathering of the parent rocks (*Bonifacio, Falsone & Piazza, 2010*). The pollution
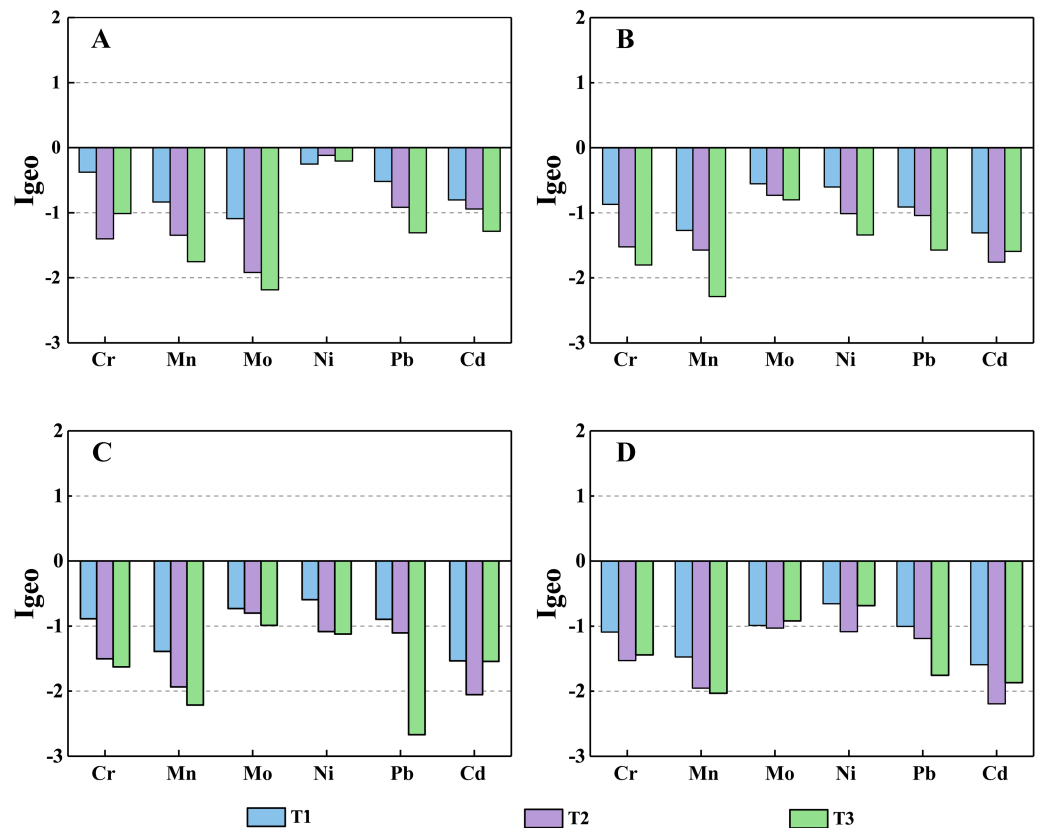
Figure 6 The I_{geo} values of HMs in three profiles at the depth of the 0–10 cm (A), 10–20 cm (B), 20–30 cm (C), and 30–50 cm (D).
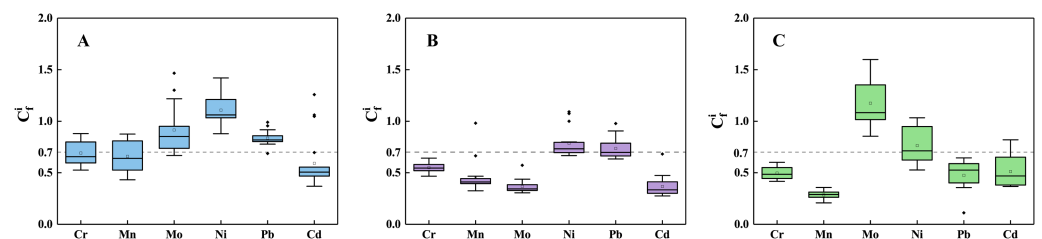
Figure 7 The contaminated factor of six HMs in the three profiles, including T1 profile (A), T2 profile (B), T3 profile (C).

phenomenon that the high Ni concentrations in soils possibly resulted from the high background value of bedrock.

The enrichment of Mo in the surface layer of the T1 profile under secondary forest may be due to the plant uptake of Mo from subsurface soils (*Brun et al., 2008*) and return into surface soils through the plant litter fall (*Marks et al., 2015*). As the only profile where the C_c^i values of almost all soils are greater than 1, the T3 profile may have received exogenous HMs input. The T3 profile has experienced intensive human activity (5-year
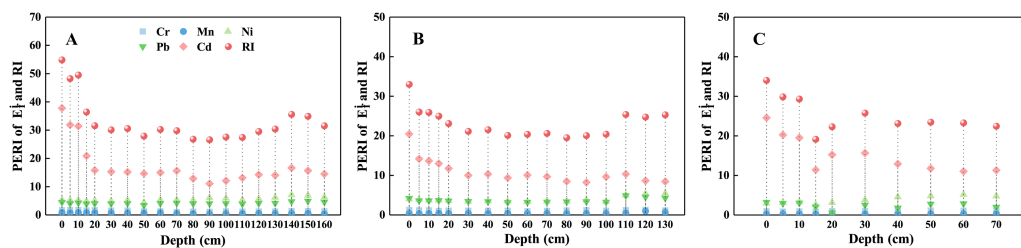
Figure 8 The potential ecological risks index of HMs in the three profiles, including T1 profile (A), T2 profile (B), T3 profile (C).

grazing period) in recent years. Mo is often added into the feed, and most of Mo ingested by animals will be excreted with feces (*Gooneratne et al., 1989*; *Ivan & Veira, 1985*). Therefore, the animal feces may have more Mo which may migrate into deeper layers as a result of leaching processes. The result showed that only two C_c^i values of Ni are higher than 1 in the T2 profile (the value in 110–120 cm: 1.07, the value in 120–130 cm: 1.09), which might be attributed to the leaching and accumulation (*Domergue & Védy, 1992*). It can be determined that there are no exogenous inputs of HMs in the T2 profile. The C_c^i values of Mo and Cd at the soil layer of 0–15 cm depth in the T1 profile were higher than 1, which might be derived from atmospheric deposition (*Zhang et al., 2016a*).

The comprehensive potential ecological risk index (RI) and the E_f^i value of each HMs are presented in Fig. 8. Based on the mean values of E_f^i, the values of HMs follow the sequence: Cd > Ni > Pb > Cr > Mn in theT1 and T3 profiles, and Ni > Pb > Cd > Cr > Mn in the profile T2. According to the classification of RI from *Hakanson (1980)*, the ecological risk in Yinjiang County soils is slight (RI < 60). Therefore, the overall quality of research profiles in the Yinjiang County is relatively safe. The management of land-use types in the study area is reasonable and the soil potential ecological risk is low.

CONCLUSIONS

The HMs (Mn, Ni, Cr, Pb, Cd and Mo) concentrations were higher in the secondary forest land and those of abandoned cropland were higher than shrubland except Mo. The dominant influence factor of the distributions of most HMs may be the soil pH and SOC. The EF values of most samples were lower than 2 and the I_{geo} values were lower than 0 in the three profiles. This possibly indicates that the main source of HMs in study area is parent rocks instead of human activities. Results from PERI on the pollution degree and the potential ecological risk are also revealed that the quality of soils in the Yinjiang County is relatively safe. However, there is no great ecological risk under reasonable management. The multiple geographic analyses (I_{geo}, C_c^i and RI) of these HMs denoted the low ecological risk of the three profiles in the Yinjiang County. In addition, through the regulation of soil pH and the content of SOC, the content of HMs in soil can be controlled.

ACKNOWLEDGEMENTS

The authors thank Dr. Yang Tang from Institute of Geochemistry, Chinese Academy of Sciences for field sampling; Dr. Qian Zhang from Institute of Geographic Sciences and Natural Resources Research, Chinese Academy of Sciences for laboratory analysis; Undergraduate innovation practice training program of Chinese Academy of Sciences.

Funding

This work was supported jointly by the Strategic Priority Research Program of Chinese Academy of Sciences (Grant No. XDB26020502) and the National Natural Science Foundation of China (Grant Nos. 41772380 and 41673020). The funders had no role in study design, data collection and analysis, decision to publish, or preparation of the manuscript.

Grant Disclosures

The following grant information was disclosed by the authors:
Chinese Academy of Sciences: XDB26020502.
The National Natural Science Foundation of China: 41772380, 41673020.

Competing Interests

The authors declare there are no competing interests.

Author Contributions

- Ruiyin Han conceived and designed the experiments, performed the experiments, analyzed the data, prepared figures and/or tables, authored or reviewed drafts of the paper, and approved the final draft.
- Zhifang Xu conceived and designed the experiments, performed the experiments, authored or reviewed drafts of the paper, and approved the final draft.

Data Availability

  The raw measurements are available in the Supplementary Files.

Supplemental Information

Supplemental information for this article can be found online at http://dx.doi.org/10.7717/peerj.12716#supplemental-information.

REFERENCES

Aboubakar A, Douaik A, Mewouo YCM, Madong RCBA, Dahchour A, El Hajjaji S. 2021. Determination of background values and assessment of pollution and ecological risk of heavy metals in urban agricultural soils of Yaoundé, Cameroon. *Journal of Soils and Sediments* **21**:1437–1454 DOI 10.1007/s11368-021-02876-4.
Ackermann F. 1980. A procedure for correcting the grain size effect in heavy metal analyses of estuarine and coastal sediments. *Environmental Technology Letters* **1**:518–527 DOI 10.1080/09593338009384008.

Allaire SE, Gupta SC, Nieber J, Moncrief JF. 2002. Role of macropore continuity and tortuosity on solute transport in soils: 2. Interactions with model assumptions for macropore description. *Journal of Contaminant Hydrology* **58**:283–298 DOI 10.1016/S0169-7722(02)00034-7.

Balabane M, Faivre D, van Oort F, Dahmani-Muller H. 1999. Mutual effects of soil organic matter dynamics and heavy metal sfate in a metallophyte grassland. *Environmental Pollution* **105**:45–54 DOI 10.1016/S0269-7491(98)00209-7.

Barbieri M. 2016. The importance of enrichment factor (EF) and geoaccumulation index (Igeo) to evaluate the soil contamination. *Journal of Geology & Geophysics* **5**:237–240 DOI 10.4172/2381-8719.1000237.

Bashir H, Ahmad K, Khan ZI. 2020. Level and speciation of nickel in some forages in relation to spatial and temporal fluctuations. *Environmental Science and Pollution Research* **27**:23793–23800 DOI 10.1007/s11356-020-08321-2.

Blaser P, Zimmermann S, Luster J, Shotyk W. 2000. Critical examination of trace element enrichments and depletions in soils: As, Cr, Cu, Ni, Pb, and Zn in Swiss forest soils. *The Science of Total Environment* **249**:257–280 DOI 10.1016/s0048-9697(99)00522-7.

Bonifacio E, Falsone G, Piazza S. 2010. Linking Ni and Cr concentrations to soil mineralogy: does it help to assess metal contamination when the natural background is high? *Journal of Soils and Sediments* **10**:1475–1486 DOI 10.1007/s11368-010-0244-0.

Brun CB, Åström ME, Peltola P, Johansson M-B. 2008. Trends in major and trace elements in decomposing needle litters during a long-term experiment in Swedish forests. *Plant and Soil* **306**:199–210 DOI 10.1007/s11104-008-9572-x.

Brusseau ML, Rao PSC. 1990. Modeling solute transport in structured soils: a review. *Geoderma* **46**:169–192 DOI 10.1016/0016-7061(90)90014-Z.

Chen Z, Wu P, Meng W, Zeng X. 2019. Effects of weathering of Qingxudong formation on heavy metal accumulation in soil in karst area. *Chinese Journal of Ecology* **38**:3747–3753 DOI 10.13292/j.1000-4890.201912.009.

Chimitdorzhieva GD, Nimbueva AZ, Bodeeva EA. 2012. Heavy metals (copper, lead, nickel, and cadmium) in the organic part of gray forest soils in the Buryat Republic. *Eurasian Soil Science* **45**:141–146 DOI 10.1134/S1064229312020068.

China Environmental Monitoring Station (CEMS). 1990. *Background values of elements in soils of China*. Beijing: China Environmental Science Press, China Environmental Monitoring Station.

Demir A. 2021. Speciation, risk assessment and bioavailability of metals in the agricultural soils of the Göksu delta, Turkey. *Soil and Sediment Contamination* **30**:292–313 DOI 10.1080/15320383.2020.1839740.

Dijkstra EF. 1998. A micromorphological study on the development of humus profiles in heavy metal polluted and non-polluted forest soils under Scots pine. *Geoderma* **82**:341–358 DOI 10.1016/S0016-7061(97)00114-6.

Domergue FL, Védy JC. 1992. Mobility of heavy metals in soil profiles. *International Journal of Environmental Analytical Chemistry* **46**:13–23 DOI 10.1080/03067319208026993.

Dumat C, Quenea K, Bermond A, Toinen S, Benedetti MF. 2006. Study of the trace metal ion influence on the turnover of soil organic matter in cultivated contaminated soils. *Environmental Pollution* **142**:521–529 DOI 10.1016/j.envpol.2005.10.027.

Fardous A, Ahmad K, Gondal S, Khan Z, Ejaz A, Valeem EE. 2011. Assesment of iron, cobalt and manganese in soil and forage: a case study at a rural livestock farm in Sargodha, Pakistan. *Pakistan Journal of Botany* **43**:1463–1465 DOI 10.1139/B11-031.

Gao P, Fu T, Wang K, Chen K, Zeng F. 2013. Spatial heterogeneity of surface soil trace lements in a small catchment in Karst peak-cluster depression area of South China. *Chinese Journal of Ecology* **32**:2133–2139 DOI 10.13292/j.1000-4890.2013.0417.

Gooneratne SR, Chaplin RK, Trent AM, Christensen DA. 1989. Effect of tetrathiomolybdate administration on the excretion of copper, zinc, iron and molybdenum in sheep bile. *British Veterinary Journal* **145**:62–72 DOI 10.1016/0007-1935(89)90011-0.

Gregorauskiene V, Kadunas V. 2006. Vertical distribution patterns of trace and major elements within soil profile in Lithuania. *Geological Quarterly* **50**:229–237 DOI 10.1111/j.0435-3676.2006.00302.x.

Gujre N, Rangan L, Mitra S. 2021. Occurrence, geochemical fraction, ecological and health risk assessment of cadmium, copper and nickel in soils contaminated with municipal solid wastes. *Chemosphere* **271**:129573 DOI 10.1016/j.chemosphere.2021.129573.

Hakanson L. 1980. An ecological risk index for aquatic pollution control.a sedimentological approach. *Water Research* **14**:975–1001 DOI 10.1016/0043-1354(80)90143-8.

Han G, Tang Y, Liu M, Van Zwieten L, Yang X, Yu C, Wang H, Song Z. 2020. Carbon-nitrogen isotope coupling of soil organic matter in a karst region under land use change, Southwest China. *Agriculture, Ecosystems & Environment* **301**:107027 DOI 10.1016/j.agee.2020.107027.

Han R, Xu Z. 2021. Geochemical behaviors of rare earth elements (REEs) in karst soils under different land-use types: a case in yinjiang karst catchment, Southwest China. *International Journal of Environmental Research and Public Health* **18**:502 DOI 10.3390/ijerph18020502.

Harter RD, Naidu R. 1995. Role of metal-organic complexation in metal sorption by soils. In: Sparks DL, ed. *Advances in agronomy*. Cambridge: Academic Press, 219–263.

Hiernaux P, Bielders CL, Valentin C, Bationo A, Fernández-Rivera S. 1999. Effects of livestock grazing on physical and chemical properties of sandy soils in Sahelian rangelands. *Journal of Arid Environments* **41**:231–245 DOI 10.1006/jare.1998.0475.

Huang J, Li X, Yang Z, Li Q, Cui G. 2017. Effects of land use change on DIC contents and δ^{13} C DIC values of surface water in a small karst catchment in Yinjiang County, Guizhou Province. *Earth and Environment* **45**:84–90 DOI 10.14050/j.cnki.1672-9250.2017.01.011.

Huang L, Rad S, Xu L, Gui L, Song X, Li Y, Wu Z, Chen Z. 2020. Heavy metals distribution, sources, and ecological risk assessment in Huixian Wetland, South China. *Water* **12**:431 DOI 10.3390/w12020431.

Ivan M, Veira DM. 1985. Effects of copper sulfate supplement on growth, tissue concentration, and ruminal solubilities of molybdenum and copper in sheep fed low and high molybdenum diets1. *Journal of Dairy Science* **68**:891–896 DOI 10.3168/jds.S0022-03028580906-1.

Jaradat QM, Massadeh AM, Momani KA, Saleem MAAl. 2009. The spatial distribution of Pb, Cd, Zn, and Cu in agricultural roadside Soils. *Soil and Sediment Contamination: An International Journal* **19**:58–71 DOI 10.1080/15320380903390554.

Khanal BR, Shah SC, Sah SK, Shriwastav CP, Acharya BS. 2014. Heavy metals accumulation in cauliflower (Brassica Oleracea L. var. Botrytis) grown in brewery sludge amended sandy loam soil. *International Journal of Agricultural Science and Technology* **2**:87–92 DOI 10.14355/ijast.2014.0203.01.

Knechtenhofer LA, Xifra IO, Scheinost AC, Flühler H, Kretzschmar R. 2003. Fate of heavy metals in a strongly acidic shooting-range soil: small-scale metal distribution and its relation to preferential water flow. *Journal of Plant Nutrition and Soil Science* **166**:84–92 DOI 10.1002/jpln.200390017.

Kong J, Guo Q, Wei R, Strauss H, Zhu G, Li S, Song Z, Chen T, Song B, Zhou T, Zheng G. 2018. Contamination of heavy metals and isotopic tracing of Pb in surface and profile soils in a polluted farmland from a typical karst area in southern China. *Science of the Total Environment* **637**:1035–1045 DOI 10.1016/j.scitotenv.2018.05.034.

Lago-Vila M, Rodríguez-Seijo A, Arenas-Lago D, Andrade L, Vega MFA. 2017. Heavy metal content and toxicity of mine and quarry soils. *Journal of Soils and Sediments* **17**:1331–1348 DOI 10.1007/s11368-016-1354-0.

Li C. 2018. Study on the growth path and Ideal state of forest coverage in Yinjiang County. *Journal of Green Science and Technology* **09**:199–200 DOI 10.16663/j.cnki.lskj.2018.09.089.

Li X, Han G, Liu M, Liu J, Zhang Q, Qu R. 2022. Potassium and its isotope behaviour during chemical weathering in a tropical catchment affected by evaporite dissolution. *Geochimica et Cosmochimica Acta* **316**:105–121 DOI 10.1016/j.gca.2021.10.009.

Li X, Han G, Zhang Q, Miao Z. 2020. An optimal separation method for high-precision K isotope analysis by using MC-ICP-MS with a dummy bucket. *Journal of Analytical Atomic Spectrometry* **35**:1330–1339 DOI 10.1039/D0JA00127A.

Liu B, Ai S, Guo R, Ren L, Zhang W, Zhang Y. 2016a. Chemical fractions and mobility of Cd, Cu, Pb and Zn in soil profile of a sewage irrigation area, Northwest China. *Journal of Residuals Science and Technology* **13**:S13–S20 DOI 10.12783/issn.1544-8053/13/S1/3.

Liu M, Han G, Li X. 2021. Using stable nitrogen isotope to indicate soil nitrogen dynamics under agricultural soil erosion in the Mun River basin, Northeast Thailand. *Ecological Indicators* **128**:107814 DOI 10.1016/j.ecolind.2021.107814.

Liu W, Liu C, Brantley SL, Xu Z, Zhao T, Liu T, Yu C, Xue D, Zhao Z, Cui L, Zhang Z, Fan B, Gu X. 2016b. Deep weathering along a granite ridgeline in a subtropical climate. *Chemical Geology* **427**:17–34 DOI 10.1016/j.chemgeo.2016.02.014.

Liu W, Liu C, Zhao Z, Xu Z, Liang C, Li L, Feng J. 2013. Elemental and strontium isotopic geochemistry of the soil profiles developed on limestone and sandstone in karstic terrain on Yunnan-Guizhou Plateau, China: implications for chemical weathering and parent materials. *Journal of Asian Earth Sciences* **67-68**:138–152 DOI 10.1016/j.jseaes.2013.02.017.

Liu Z, Nie Y, Zhang L, Wang Z, Bai Q, Yang C. 1990. Translocation and transformation of heavy metals in water logged aeration zone of soil. *Acta Scientiae Circumstantiae* **02**:160–172 DOI 10.13671/j.hjkxxb.1990.02.006.

Markiewicz-Patkowska J, Hursthouse A, Przybyla-Kij H. 2005. The interaction of heavy metals with urban soils: sorption behaviour of Cd, Cu, Cr, Pb and Zn with a typical mixed brownfield deposit. *Environment International* **31**:513–521 DOI 10.1016/j.envint.2004.09.004.

Marks JA, Perakis SS, King EK, Pett-Ridge J. 2015. Soil organic matter regulates molybdenum storage and mobility in forests. *Biogeochemistry* **125**:167–183 DOI 10.1007/s10533-015-0121-4.

Mazurek R, Kowalska J, Gąsiorek M, Zadrozny P, Józefowska A, Zaleski T, Kępka W, Tymczuk M, Orłowska K. 2017. Assessment of heavy metals contamination in surface layers of Roztocze National Park forest soils (SE Poland) by indices of pollution. *Chemosphere* **168**:839–850 DOI 10.1016/j.chemosphere.2016.10.126.

Muller G. 1969. Index of geoaccumulation in sediments of the Rhine river. *GeoJournal* **2**:109–118.

Müller G. 1971. Schwermetalle in den sedimenten des Rheins-Veräderungen seit. *Umschau* **79**:778–783.

Nazeer S, Hashmi MZ, Malik RN. 2014. Heavy metals distribution, risk assessment and water quality characterization by water quality index of the River Soan, Pakistan. *Ecological Indicators* **43**:262–270 DOI 10.1016/j.ecolind.2014.03.010.

Office of Solid Waste and Emergency Response. 1993. *Draft soil screening guidance.* Washington: Nation Service Center for Environmental Publications.

Ottosen LM, Hansen HK, Jensen PE. 2009. Relation between pH and desorption of Cu, Cr, Zn, and Pb from industrially polluted soils. *Water, Air, and Soil Pollution* **201**:295–304 DOI 10.1007/s11270-008-9945-z.

Parise M, De Waele J, Gutierrez F. 2009. Current perspectives on the environmental impacts and hazards in karst. *Environmental Geology* **58**:235–237 DOI 10.1007/s00254-008-1608-2.

Probst A, Hernandez L, Probst JL, Ulrich E. 2003. Heavy metals in some French forest soils: distribution, origin and controlling factors. *Journal de Physics Archives* **107**:1107–1110 DOI 10.1051/jp4:20030494.

Qiu J, Fu J, Fu S, Xiao F, Wang D, Chang X. 2016. Spatial distribution and potential ecological risk assessment of heavy metals in cultivated soil profiles of Hengshi

River Basin in the sulfide mine, Northern Guangdong. *Ecological Science* **35**:56–64 DOI 10.14108/j.cnki.1008-8873.2016.03.009.

Reimann C, Caritat Pd. 2000. Intrinsic flaws of element enrichment factors (EFs) in environmental geochemistry. *Environmental Science & Technology* **34**:5084–5091 DOI 10.1021/es001339o.

Rieuwerts JS, Thornton I, Farago ME, Ashmore MR. 1998. Factors influencing metal bioavailability in soils: preliminary investigations for the development of a critical loads approach for metals. *Chemical Speciation & Bioavailability* **10**:61–75 DOI 10.3184/095422998782775835.

Rudnick RL, Gao S. 2003. Composition of the continental Crust. Treatise on geochemistry 3:1-64. In: Holland HD, Turekian KK, eds. *Treatise on geochemistry*. Oxford: Elsevier, 1–64.

Sauvé S, McBride M, Hendershot W. 1997. Soil solution speciation of Lead(II): effects of organic matter and pH. *Soil Science Society of America Journal* **62**:618–621 DOI 10.2136/sssaj1998.03615995006200030010x.

Sawut R, Kasim N, Maihemuti B, Hu L, Abliz A, Abdujappar A, Kurban M. 2018. Pollution characteristics and health risk assessment of heavy metals in the vegetable bases of northwest China. *Science of the Total Environment* **642**:864–878 DOI 10.1016/j.scitotenv.2018.06.034.

Semerjian L, Ayoub GM. 2003. High-pH–magnesium coagulation–flocculation in wastewater treatment. *Advances in Environmental Research* **7**:389–403 DOI 10.1016/S1093-01910200009-6.

Skierszkan EK, Mayer KU, Weis D, Beckie RD. 2016. Molybdenum and zinc stable isotope variation in mining waste rock drainage and waste rock at the Antamina mine, Peru. *Science of the Total Environment* **550**:103–113 DOI 10.1016/j.scitotenv.2016.01.053.

Soil Survey Staff. 2010. Keys to soil taxonomy, 11th edition. Washington, DC: U.S. Department of Agriculture, Natural Resources Conservation Service.

Sparks DL. 2003. *Environmental soil chemistry: second edition*. Academic Press.

Sun Y, Zhou Q, Xie X, Liu R. 2010. Spatial, sources and risk assessment of heavy metal contamination of urban soils in typical regions of Shenyang, China. *Journal of Hazardous Materials* **174**:455–462 DOI 10.1016/j.jhazmat.2009.09.074.

Tao H, Liao X, Li Y, Xu C, Zhu G, Cassidy DP. 2020. Quantifying influences of interacting anthropogenic-natural factors on trace element accumulation and pollution risk in karst soil. *Science of the Total Environment* **721**:137770 DOI 10.1016/j.scitotenv.2020.137770.

Taylor MP, Mackay AK, Hudson-Edwards KA, Holz E. 2010. Soil Cd, Cu, Pb and Zn contaminants around Mount Isa city, Queensland, Australia: potential sources and risks to human health. *Applied Geochemistry* **25**:841–855 DOI 10.1016/j.apgeochem.2010.03.003.

TBS. 2017. *Tongren statistical yearbook*. Pubish House of Local Records: Tongren Bureau of Statistics.

Vodyanitskii YN, Yakovlev AS. 2011. Assessment of soil contamination by the content of heavy metals in the soil profile. *Eurasian Soil Science* **44**:297–303 DOI 10.1134/S1064229311010169.

Wang L, Zhang M. 2007. Release behaviors of heavy metals from polluted soils with heavy metals of different sources. *Research of Environmental Sciences* **04**:134–138 DOI 10.13198/j.res.2007.04.138.wanglp.025.

Wei B, Yang L. 2010. A review of heavy metal contaminations in urban soils, urban road dusts and agricultural soils from China. *Microchemical Journal* **94**:99–107 DOI 10.1016/j.microc.2009.09.014.

Wen Y, Li W, Yang Z, Zhuo X, Guan D-X, Song Y, Guo C, Ji J. 2020. Evaluation of various approaches to predict cadmium bioavailability to rice grown in soils with high geochemical background in the karst region, Southwestern China. *Environmental Pollution* **258**:113645 DOI 10.1016/j.envpol.2019.113645.

Wu H, Liu Q, Ma J, Liu L, Qu Y, Gong Y, Yang S, Luo T. 2020. Heavy Metal(loids) in typical Chinese tobacco-growing soils: concentrations, influence factors and potential health risks. *Chemosphere* **245**:125591 DOI 10.1016/j.chemosphere.2019.125591.

Xiao R, Wang S, Li R, Wang JJ, Zhang Z. 2017. Soil heavy metal contamination and health risks associated with artisanal gold mining in Tongguan, Shaanxi, China. *Ecotoxicology and Environmental Safety* **141**:17–24 DOI 10.1016/j.ecoenv.2017.03.002.

Xu P, An Q, Ding L, Zhang G, Luo H. 2017a. Dynamic analysis of land use change in Yinjiang County from 2010 to 2015. *Journal of Green Science and Technology* 211–212+215 DOI 10.16663/j.cnki.lskj.2017.18.073.

Xu Z, Ni S, Tuo X, Zhang C. 2008. Calculation of heavy metals' toxicity coefficient in the evaluation of potential ecological risk index. *Environmental Science & Technology* **02**:112–115 DOI 10.19672/j.cnki.1003-6504.2008.02.030.

Xu Y, Zhou X, Zhao C, Yang J, Niu Q. 2017b. Ecological security pattern construction in Yinjiang watershed based on Karst vulnerability assessment. *Journal of Guizhou Normal University (Natural Sciences)* **35**:22–29 DOI 10.16614/j.cnki.issn1004-5570.2017.06.004.

Yang H, Zhu T, Wang X, Pu J, Li J, Zhang T, Cao J. 2018. Soil element contents of typical small watershed in the plateau area of karst fault Basin, Yunnan. *Ecology and Environment Sciences* **27**:859–865 DOI 10.16258/j.cnki.1674-5906.2018.05.009.

You M, Huang Y, Lu J, Li C. 2015. Fractionation characterizations and environmental implications of heavy metal in soil from coal mine in Huainan, China. *Environmental Earth Sciences* **75**:78 DOI 10.1007/s12665-015-4815-7.

Zeng J, Han G, Yang K. 2020. Assessment and sources of heavy metals in suspended particulate matter in a tropical catchment, northeast Thailand. *Journal of Cleaner Production* **265**:121898 DOI 10.1016/j.jclepro.2020.121898.

Zhang M. 2005. Preferential transfer of the heavy metals in the polluted soils. *Acta Scientiae Circumstantiae* **02**:192–197 DOI 10.13671/j.hjkxxb.2005.02.011.

Zhang Q, Han G, Liu M, Liang T. 2019. Spatial distribution and controlling factors of heavy metals in soils from Puding Karst Critical Zone Observatory, southwest China. *Environmental Earth Sciences* **78**:279.271–279.213 DOI 10.1007/s12665-019-8280-6.

Zhang J, Li H, Zhou Y, Dou L, Cai L, Mo L, You J. 2018. Bioavailability and soil-to-crop transfer of heavy metals in farmland soils: a case study in the Pearl River Delta, South China. *Environmental Pollution* **235**:710–719 DOI 10.1016/j.envpol.2017.12.106.

Zhang Y, Zhang M, Niu J, Zheng H. 2016b. The preferential flow of soil: a widespread phenomenon in pedological perspectives. *Eurasian Soil Science* **49**:661–672 DOI 10.1134/S1064229316060120.

Zhang G, Zhao Q, Jia J, Wen X. 2016a. Heavy metals pollution in soil profiles from seasonal-flooding riparian wetlands in a Chinese Delta: levels, distributions and toxic risks. *Physics and Chemistry of the Earth, Parts A/B/C* **97**:54–61 DOI 10.1016/j.pce.2016.11.004.

Zhao F-J, Ma Y, Zhu Y-G, Tang Z, McGrath SP. 2015. Soil contamination in China: current status and mitigation strategies. *Environmental Science & Technology* **49**:750–759 DOI 10.1021/es5047099.

Zoller WH, Gladney ES, Duce RA. 1974. Atmospheric concentrations and sources of trace metals at the South pole. *Science* **183**:198–200 DOI 10.1126/science.183.4121.198.